J. Mol. Model. **1997**, *3*, 434 – 442

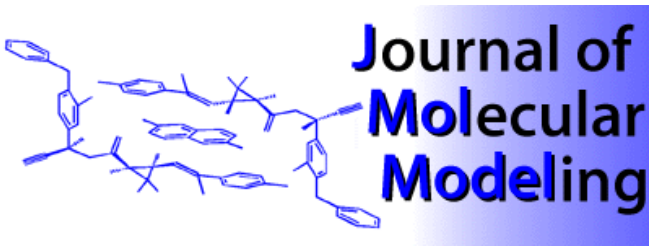

The Hydrolysis Mechanism of Formamide Revisited: Comparison Between ab initio, Semiempirical and DFT Results

Serge Antonczak, Manuel Ruiz-López*, and Jean-Louis Rivail

Laboratoire de Chimie Théorique, URA CNRS 510, Institut Nancéien de Chimie Moléculaire, Université Henri Poincaré, Nancy I. BP 239, F-54506 Vandœuvre-lès-Nancy Cedex, France; Tel. +33-3-8391-2527; Fax: +33-3-8391-2530 (ruiz@lctn.u-nancy.fr)

Received: 2 July 1997 / Accepted: 21 October 1997 / Published: 30 October 1997

Abstract

The hydrolysis of amides is a model reaction to study peptide hydrolysis. This process has been previously considered in the literature at the ab initio level. In this work, we revisit different reaction mechanisms (water-assisted, non-assisted, neutral and acid-catalyzed) with various theoretical methods : semiempirical, ab initio and Density Functional. The ab initio calculations are carried out at a computational level which is substantially higher than in previous studies. We describe the structure of the transition states and discuss the influence of the catalyst. We also compute the activation free energies for these processes at the Density Functional Theory level. Comparison of the methods allows to outline the main trends of these theoretical approaches which may be useful to design new computational strategies for investigating biological reaction mechanisms through the use of combined Quantum Mechanics/Molecular Mechanics methods.

Keywords : Amides, Hydrolysis, Reaction mechanism, Peptides, Theoretical calculations

Introduction

The hydrolysis of formamide is a reaction of primary importance since it can be considered as a model for the cleavage of peptidic bonds (see Scheme 1 for a schematic representation of the process). Theoretical effort has been devoted to study this reaction [1-5] or related processes [6]. In a previous work [4], we have studied the influence of bifunctional catalysis (herein noted water-assisted or assisted mechanisms) and acid-catalysis using ab initio schemes of computation. RHF/3-21G [7] was the level used for geometry optimisations. Energy calculations were performed taking into account the effect of correlation energy. Solvent effects were also taken into account. In that work, we focused our attention on the first step of the hydrolysis which consists in a concerted protonation of the N atom and the hydroxylation of the C atom of formamide. In water-assisted mechanism, an additional water molecule plays the role of a proton relay catalyst. The reaction proceeds through the breaking of the CN bond but this step is not the rate-limiting stage of the reaction.

Obviously, the study of the hydrolysis mechanism in biological processes cannot be made with standard quantum chemistry procedures. An interesting perspective is offered by the use of hybrid Quantum Mechanics and Molecular Mechanics (QM/MM) methods which combine the quantum description of the reactive part of the system with a classical

* *To whom correspondence should be addressed*

Table 1. *Geometrical parameters (bondlengths in Å and angles in degrees) and total energies (in a.u.) at several levels of computation for the transition state of the neutral non-assisted mechanism. Modifications with respect to isolated formamide parameters are presented in parenthesis.*

	TS1N		
Geometrical Parameters	**AM1**	**MP2/6-31G****	**BLYP/6-31G****
C_1O_1	1.265 (+0.022)	1.221 (-0.002)	1.220 (-0.009)
C_1N_1	1.521 (+0.154)	1.586 (+0.226)	1.664 (+0.291)
C_1O_2	1.582	1.788	1.854
O_2H_1	1.294	1.322	1.359
H_1N_1	1.219	1.181	1.190
$N_1C_1O_2$	87.17	83.10	81.59
$H_1O_2C_1$	81.58	68.89	68.93
$N_1C_1O_2H_1$	-2.01	-6.00	-4.67
Total energies	-38.337167	-245.589898	-246.198272

treatment of the remaining atoms. Most of the present applications of this technique are being done at the semiempirical level [8] although hybrid Density Functional Theory (DFT) [9] and ab initio methods [10] are also being developed.

However, it is well known that in the theoretical description of chemical reactions the results may be quite dependent on the computational level. For this reason, a detailed study of model systems with accurate ab initio calculations is suitable prior to application of approximate methods to investigate very large species. This is our aim in the present paper.

We present below a study of assisted and non-assisted mechanisms of hydrolysis of formamide in neutral or acid-catalyzed conditions with several methods of computation (ab initio, DFT and semiempirical). Application of QM/MM methods to the study of peptide hydrolysis catalyzed by thermolysin will be reported in due course [11]. Comparison of DFT with ab initio [12] or experimental [13] results has been done for different systems and the DFT approach has been shown to be suitable for studying metal containing molecules [14].

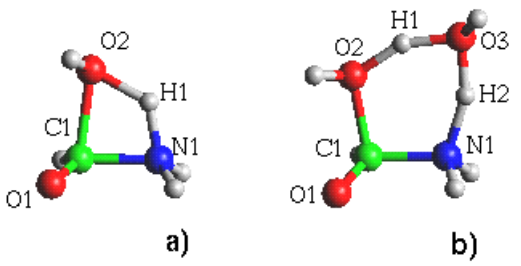

Figure 1. *Structures corresponding to the transition states for the neutral non-assited mechanism (a), water-assisted mechanism (b).*

Method of computation

Ab initio and DFT calculations have been carried out using the Gaussian92/DFT [15] package. The influence of the computational level (*ab initio*, DFT) on the amide hydrolysis reaction enthalpies has been studied in detail [5]. It was shown that a very extended basis set (at least triple-z with polariza-

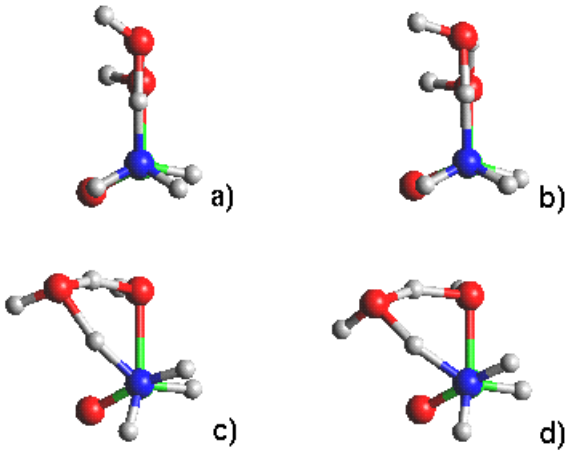

Figure 2. *Transition states corresponding to the neutral water-assisted mechanism shown in Newman projection at several levels of computation: a) RHF/3-21G, b) AM1, c) BLYP/6-31G**, d) MP2/6-31G**.*

Table 2. *Geometrical parameters (bondlengths in Å and angles in degrees) and total energies (in a.u.) at several levels of computation for the transition state of the neutral assisted mechanism. Modifications with respect to isolated formamide parameters are presented in parenthesis.*

	TS2N		
Geometrical Parameters	**AM1**	**MP2/6-31G****	**BLYP/6-31G****
C_1O_1	1.277 (+0.034)	1.238 (+0.015)	1.230 (+0.001)
C_1N_1	1.512 (+0.145)	1.527 (+0.167)	1.587 (+0.214)
C_1O_2	1.558	1.747	1.862
O_2H_1	1.300	1.295	1.295
H_1O_3	1.141	1.174	1.174
O_3H_2	1.167	1.192	1.297
H_2N_1	1.403	1.312	1.245
$O_1C_1N_1$	113.96	115.18	114.58
$O_2C_1N_1$	106.55	93.33	115.17
$H_1O_2C_1$	117.46	93.94	97.09
$O_3H_1O_2$	140.19	156.37	158.78
$H_2O_3H_1$	97.02	84.22	83.27
$N_1H_2O_3$	152.78	155.23	157.99
$H_NC_1N_1H_N$'	–122.38	–120.18	–120.74
$N_1C_1O_2H_1$	1.65	–56.47	–46.98
$C_1O_2H_1O_3$	–12.80	30.37	33.03
$O_2H_1O_3H_2$	14.21	7.11	–3.27
$H_1O_3H_2N_1$	–10.08	–15.47	–2.72
Total energies	–51.152029	–321.826978	–322.628804

tion functions) and high level correlation methods (MP4, QCISD) must be used in order to obtain accurate properties. Since such methods cannot be used for large systems, we decided here to use an intermediate level. The 6-31G** [16] basis set has been employed. The influence of diffuse function will be illustrated in some cases. The second order Møller-Plesset [17] (MP2) theory was used to assess the influence of electron correlation. The DFT calculations have been performed using the BLYP functional which employs Becke's exchange functional [18] and Lee-Yang-Parr correlation functional [19]. Becke's functional is a density gradient corrected Slater exchange. The Lee-Yang-Parr correlation functional also includes density gradient corrections. The BLYP approach has been extensively employed in the literature [20]. The semiempirical computations have been performed with the GEOMOS [21] program, using the AM1 [22] method. The geometry of the stationary points has been fully optimized at these different levels of calculation.

The transition states have been located using Schlegel's algorithm [23] and characterized by Hessian matrix calculations, verifying that it presents only one negative eigenvalue corresponding to an imaginary frequency. Free energy computations were made using standard procedures [24].

The following short notations are employed below : MP2 holds for MP2/6-31G** calculations ; BLYP holds for BLYP/6-31G** computations ; A//B means that a single point energy calculation at level A has been done using the optimized geometry obtained at level B of computation.

Results and discussion

The hydrolysis of formamide is studied here for neutral and acid-catalyzed reactions. For each process, water-assisted and non-assisted mechanisms are considered. Hence four different reactions will be described here. Only the reactants and the transition states have been computed since it has been shown in a previous work [4] that reaction intermediates appearing in the potential energy surface are not stable when considering the free energy surface. In our study for the acid-catalyzed reaction, we have assumed that the oxygen of the carbonyl group of formamide is bonded to H_3O^+. Indeed, it has been shown that, despite of the fact that N-protonated

Table 3. *Geometrical parameters (bondlengths in Å and angles in degrees) and total energies (in a.u.) at several levels of computation for the transition state of the acid-catalyzed non-assisted mechanism. Modifications with respect to protonated-formamide parameters are presented in parenthesis.*

	TS1P		
Geometrical Parameters	**AM1**	**MP2/6-31G****	**BLYP/6-31G****
C_1O_1	1.382 (+0.045)	1.331 (+0.053)	1.326 (+0.039)
C_1N_1	1.468 (+0.148)	1.468 (+0.144)	1.495 (+0.176)
C_1O_2	1.468	1.545	1.617
O_2H_1	1.286	1.180	1.321
H_1N_1	1.443	1.359	1.347
$N_1C_1O_2$	91.74	91.23	89.83
$H_1O_2C_1$	86.34	77.32	75.66
$N_1C_1O_2H_1$	-0.89	-6.45	-5.09
Total energies	-51.452073	-322.215817	-322.992519

formamide is 14 kcal·mol^{-1} more stable than O-protonated one, the hydrolysis is easier in the latter case. One may note however that in the case of strained amides, N-protonation may be favored [5b]. As a starting point to locate the transition states, the geometry of the structure described in previous work [4] has been used. Finally, note that we do not take into account interactions with other solvent molecules. Actually, one may expect that hydrogen bonding of a solvent water molecule with the carbonyl oxygen on the formamide molecule would lead to a mechanism intermediate between the neutral and the acid-catalyzed ones. Long-range electrostatic effects on this reaction have been analysed before [4] and do not play a major role. The following notations will be used for the transition states : TS1N and TS2N will hold for neutral non-assisted and neutral water-assisted reactions respectively; TS1P and TS2P will hold for acid-catalyzed non-assisted and acid-catalyzed water-assisted reactions respectively.

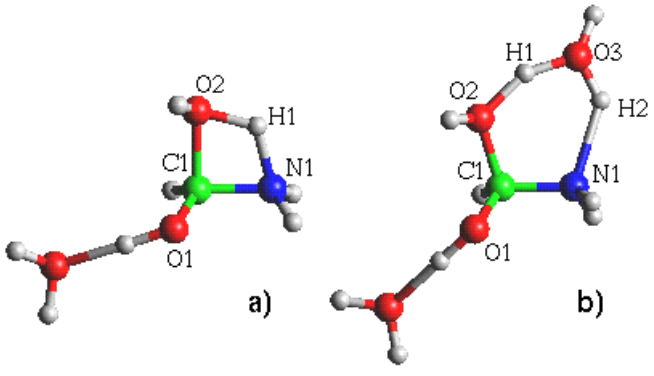

Figure 3. *Structures corresponding to the transition states for the acid-catalyzed non-assited mechanism (above), water-assisted mechanism (below).*

Structures and total energies

Geometrical parameters and total energies corresponding to the non-catalyzed reactions are summarized in Table 1 (non-assisted mechanism) and in Table 2 (water-assisted mechanism). The corresponding quantities for the acid-catalyzed processes are compiled in Table 3 (non-assisted mechanism) and in Table 4 (water-assisted mechanism). In Figure 1, the structures of the neutral mechanism are schematically represented and the atoms are numbered. In Figure 2, we compare the structures of the water-assisted neutral mechanism TS's obtained with several computational methods. Figures 3 and 4 contain the same informations for the acid-catalyzed processes.

Non-assisted neutral mechanism. AM1, MP2 and BLYP computations predict a transition state in which there is a four membered ring (Figure 1a). Although the structures obtained at the different levels are qualitatively similar, some noticeable differences exist. At the DFT level, the forming C_1O_2 bondlength is a little larger than that obtained at the ab initio level whereas the corresponding value obtained at the AM1 level is substantially shorter. However, it must be pointed out that DFT calculations leads to larger modification of the C_1N_1 bond of formamide compared to ab initio results. In semiempirical calculations, the increase of C_1N_1 bond is less important. For the other forming bond, H_1N_1, the three methods give comparable results although the calculated AM1 bondlength is slightly larger. The ab initio values may be compared to those previously obtained at the RHF/3-21G level

Table 4. *Geometrical parameters (bondlengths in Å and angles in degrees) and total energies (in a.u.) at several levels of computation for the transition state of the catalyzed assisted mechanism. Modifications with respect to protonated-formamide parameters are presented in parenthesis.*

	TS2P		
Geometrical Parameters	**AM1**	**MP2/6-31G****	**BLYP/6-31G****
C_1O_1	1.398 (+0.061)	1.358 (+0.080)	1.355 (+0.068)
C_1N_1	1.447 (+0.127)	1.444 (+0.140)	1.465 (+0.146)
C_1O_2	1.460	1.501	1.567
O_2H_1	1.405	1.258	1.261
H_1O_3	1.095	1.153	1.192
O_3H_2	0.998	0.996	1.027
H_2N_1	2.144	1.881	1.777
$O_1C_1N_1$	112.20	114.79	112.79
$O_2C_1N_1$	108.54	112.54	106.50
$H_1O_2C_1$	115.42	110.71	109.66
$O_3H_1O_2$	154.41	162.22	160.14
$H_2O_3H_1$	106.11	95.84	92.49
$N_1H_2O_3$	121.74	132.52	139.65
$H_NC_1N_1H_N$'	123.63	–115.12	–116.15
$N_1C_1O_2H_1$	17.68	18.53	17.08
$C_1O_2H_1O_3$	16.62	–12.97	–14.79
$O_2H_1O_3H_2$	–30.47	8.94	10.43
$H_1O_3H_2N_1$	8.55	–12.30	–12.58
Total energies	–64.297076	–398.473531	–399.439970

[4]. In fact, the 3-21G basis give reasonable results. Nevertheless, proton transfer to the nitrogen atom is more advanced in the case of MP2/6-31G** results (H_1N_1 equal 1.181 Å at MP2/6-31G** and 1.219 Å at RHF/3-21G) whereas the nucleophilic attack on C_1 is slightly delayed (C_1O_2 equal 1.788 Å at MP2/6-31G** and 1.748 Å at RHF/3-21G).

To the best of our knowledge, this is the first DFT study on amide hydrolysis reaction mechanisms. Therefore, direct comparison with previous DFT results is not possible. One can observe, however, that in other processes such as pericyclic reactions [25], structural differences between DFT and MP2 computations have been discussed. In general, both methods lead to comparable bondlengths for stable species but for transition structures notable changes have been reported in some cases. Indeed, differences of ±0.1 Å are not exceptional.

Assisted neutral mechanism. In this case, the TS predicted by all the methods (see structure b in Figure 1) consists in a six-membered ring formed by the water dimer and the C_1N_1 bond. The main difference in these structures lies in the fact that MP2 and BLYP calculations, in contrast with AM1, lead to a non-planar six membered ring (see Figure 2). Rotations of the amino group around C_1N_1 bond is substantial as can be illustrated using the $H_2N_1C_1O_2$ dihedral angle : 54.0° for MP2 and 47.0° for BLYP calculations. Previous results at the RHF/3-21G level predicted, as AM1, an almost planar ring. In order to elucidate the role of electron correlation and basis set, we have also located this transition state at the RHF/6-31G** level. In this case, the $H_2N_1C_1O_2$ angle is 50.8° showing that the ring conformation of this transition state exhibits a substantial basis set dependence.

MP2 and BLYP calculations present the same trends than those remarked before for the non-assisted mechanism. Note for instance the larger C_1O_2 bondlength in the case of BLYP (see Table 3). Note also that proton transfer in the TS is favoured by BLYP calculations with respect to MP2 ones. More important differences are found when these methods are compared to AM1. In particular, the semiempirical calculations lead to a more asynchronous reaction. That is, the proton transfer between water molecules is more advanced that in either MP2 or BLYP computations whereas the proton transfer to the nitrogen atom is delayed. Finally, as in the non-

assisted mechanism, the forming C_1O_2 bond is much shorter with the AM1 method.

As said above, structural differences between MP2 and DFT for transition structures, especially for bonds participating to the transition vector, are comparable to those obtained for other reactions [25]. Note that in TS2N, there are two proton transfers. Proton transfer reactions in multiple hydrogen bond systems have been studied at the DFT level and compared to MP2 results [26] showing also that at the transition states, substantial differences may exist between the lengths of the bonds being formed. DFT studies on the cooperative effect due to hydrogen bond formation in water clusters have been also reported [27].

Non-assisted acid-catalyzed mechanism. The three methods predict a four membered ring almost planar (see structure a in Figure 3 and values in Table 3). Comparisons of this process with the non-assisted neutral mechanism shows that all the methods predict a shorter C_1O_2 bondlength and a longer H_1N_1 one. Note that the C_1O_1 bond is longer in this case (Table 3) which is due to the stabilisation of the H_2N^+=CH-O^- mesomeric form of formamide through O-protonation.

Here again, MP2 results are in agreement with previous RHF/3-21G results [4]. For instance, the predicted decrease of the C_1O_1 bondlength in going from TS1N to TS1P is comparable (1.788 Å and 1.545 Å respectively for MP2 results, 1.748 Å and 1.536 Å for RHF/3-21G results). Comparing BLYP and MP2 calculations, one may see that the structures obtained for the TS's are quite close. The main difference lies in the slightly more asymmetric reaction coordinate predicted by BLYP, which exhibits a larger late character (O_2H_1 is longer, N_1H_1 is slightly shorter and C_1O_2 slightly longer at the BLYP level).

AM1, on the contrary, displays important differences with respect to either MP2 or BLYP. Note in particular the lower asymmetry of the TS in this case.

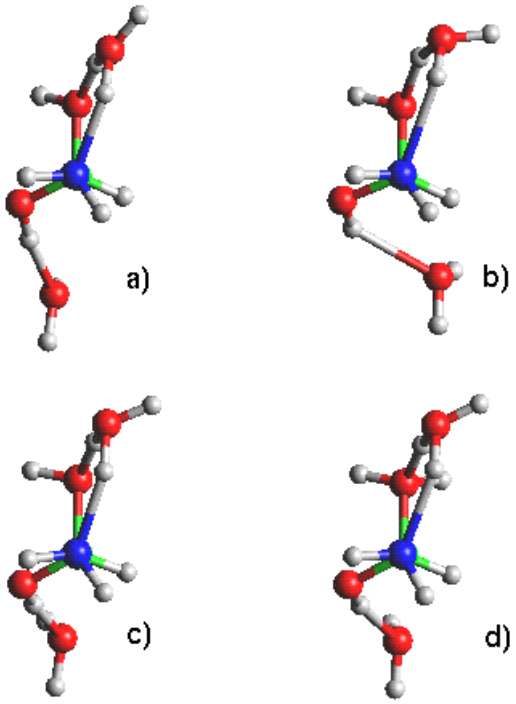

Figure 4. *Transition states corresponding to the acid-catalyzed water-assisted mechanism shown in Newman projection at several levels of computation: a) RHF/3-21G, b) AM1, c) BLYP/6-31G**, d) MP2/6-31G**.*

Assisted acid-catalyzed mechanism. The calculations predict a six-membered ring for the transition structure which is not planar (Figure 4). The rotation of the amino group is found to be in the opposite direction than that previously remarked for the neutral process at MP2 and BLYP levels (Figure 2). Note also that the rotation here is less intense, as illustrated by the $H_2N_1C_1O_2$ dihedral angle : -18.9° for BLYP, -21.2° for MP2 and -20.9° for AM1 calculations (Table 4). As shown in Figure 4, these results are close to RHF/3-21G results (-20.6°) previously reported [4]. We have tried to locate another transition state starting from structures for which the amino group rotation was made in the opposite direction. Such calculations have been made at the AM1 level only. No transition state corresponding to the cleavage of the amidic bond was found. Therefore, the direction of the rotation, *i.e.* the deviation of the planarity of the six-membered ring, seems to be directly determined by the presence or the absence of the catalyst.

As obtained for the neutral water-assisted process, the BLYP C_1O_2 bondlength is larger than the MP2 one. Note also that the proton transfer in the transition state is enhanced in BLYP calculations with respect to MP2 ones. Again the semiempirical calculations present more asynchronous proton transfers: the proton transfer towards the nitrogen atom is retarded while the proton transfer between the two water molecules has almost completely occurred. Therefore, an [H_3O^+]-like entity, involving H_1, O_3, H_2 and H_2' atoms, can be pointed out at the TS in the case of AM1 method. Finally, the C_1O_2 forming bond is shorter with AM1 method as compared to either BLYP or MP2 calculations. Nevertheless, in the water-assisted catalyzed mechanism, differences between BLYP, MP2 and AM1 results are less important than in the corresponding neutral water-assisted process.

Energetics of the reactions

Relative energies. In Table 5, we give the relative energies of the transition states for the neutral and acid catalyzed, water-assisted and non-assisted mechanisms at different levels of computation. Results presented in Table 5 are given with respect to the separate reactive molecules. Note that some of the TS relative energies are negative, *i.e.*, the potential energy at the TS is below that of the reactants. As mentioned above, it has been demonstrated in a previous work that re-

Table 5. *Relative energies (kcal·mol^{-1}) of the transition states with respect to reactants for the different mechanisms (neutral and acid-catalyzed, water-assisted and non-assisted).*

	Optimized Geometries			Single-point calculations			
	AM1	**MP2**	**BLYP**	**MP2/AM1**	**BLYP/AM1**	**MP2/BLYP**	**BLYP/MP2**
TS1N	+58.46	+40.87	+32.65	+53.89	+48.08	+41.96	+33.49
TS2N	+55.48	+31.69	+12.59	+37.36	+29.90	+22.24	+13.80
TS1P	+30.05	+26.69	+24.78	+33.50	+32.47	+27.56	+25.49
TS2P	+8.16	-7.86	-7.90	-3.21	-2.07	-6.86	-7.22

action intermediates exist before the TS's in the potential energy surface although they are unstable in the free energy surface at normal pressure and temperature conditions [4]. For this reason, they are not considered in the present work. We shall show below that when free energies are considered, all TS have positive values with respect to the reactants. In order to analyse the influence of the geometry on the computed relative energies, we have also performed a series of single-point calculations. Thus, in Table 5, MP2 and BLYP relative energies are given for each TS using the geometries optimized at the AM1, MP2 or DFT levels.

Let us first compare the results obtained using the optimized geometries. Note that for TS1P and TS2P, MP2 and BLYP give close results. However, in most cases, substantial differences appear when one compares the value for a given TS through the three computational levels. In particular, the AM1 calculations substantially overestimate all the activation energies. For TS1N and TS2N, on the contrary, BLYP energies are 10 to 20 kcal·mol^{-1} below the MP2 values. This difference is quite large and can be due to the use of limited basis sets, as pointed out by one of the referees. To check this, we have estimated the influence of diffuse functions in the basis set. Thus, single point calculations on 6-31G** geometries using the 6-31+G** basis set have been carried out to compute the activation barriers of TS1N and TS2N. The results show that the BLYP-MP2 energy difference decreases substantially although it is still of the order of 4-5 kcal·mol^{-1} in both cases (activation energies for TS1N are 43·22 kcal.mol^{-1} and 38·22 kcal·mol^{-1} at MP2 and BLYP levels respectively; for TS2N the corresponding values are 27·36 kcal.mol^{-1} and 23·56 kcal·mol^{-1}; the addition of diffuse functions on hydrogen atoms modified very slightly these values). As noted in the introduction, the use of triple-ζ basis set and refined correlation methods seems also to be necessary in order to obtain very accurate quantities for these reactions [5]. Unfortunately, such type of calculations were beyond our present capabilities.

It can be noted that all the methods show a diminution of the TS-reactants relative energy from non-assisted to assisted processes. In the case of neutral processes (TS1N and TS2N), this difference is about 20 kcal·mol^{-1} for BLYP computations while it is only 9 kcal·mol^{-1} and 3 kcal·mol^{-1} for MP2 and AM1 methods respectively. This difference is about 16 kcal·mol^{-1} for MP3/6-31G**//RHF/3-21G calculations [4] (note that this value is close to those obtained using single point computations at the MP2 and BLYP levels with the 6-31+G** basis set, as discussed above). The corresponding differences for the protonated processes (TS1P and TS2P) show larger values : about 32-33 kcal·mol^{-1} for BLYP and MP2 results and 22 kcal·mol^{-1} for AM1.

Acid catalysis is predicted by the three methods. However, significant differences can be noted and the catalytic effect follows the order AM1 > MP2 > BLYP.

It is interesting to remark that the BLYP method predict neutral bifunctional catalysis (compare TS1N and TS2N) to be larger than non-assisted acid catalysis (compare TS1N and TS1P) by about 12 kcal·mol^{-1}. In the case of MP2 and AM1 computations, the opposite trend is found (by 5 kcal·mol^{-1} at MP2 level and by 25 kcal·mol^{-1} at AM1 one).

Let us now examine the influence of the geometry on the relative energy results. We see in Table 5 that BLYP//MP2 computations give approximately the same values than BLYP. Similarly, MP2//BLYP and MP2 are close except for TS2N case. These results are not surprising since MP2 an BLYP geometries present only slight differences.

When BLYP//AM1 and MP2//AM1 are compared to BLYP and MP2 respectively, one can note that the relative energies are overestimated especially for the neutral processes. However, the calculation of the total energy with BLYP or MP2 using AM1 geometries allows to improve a little AM1 relative energy results.

Free-energy calculations. In order to obtain free energy variations along the reaction paths, we have computed thermodynamic quantities at 298°C and 1 atm following the standard procedures. Only BLYP/6-31G** calculations will be presented here and compared to MP2/6-31G**//RHF/3-21G calculations [4]. These results are summarized in Table 6.

It is well known that entropic effects are fundamental concerning the reactivity of weakly bonded complexes. In-

Table 6. *Energetics (kcal.mol^{-1}) for formamide hydrolysis reactions.*

	BLYP/6-31G**			MP2/6-31G**//RHF/3-21G
	Δ(H-E)	**-TΔS**	**ΔG**	**ΔG [a]**
TS1N	-0.46	12.45	44.64	53.00
TS2N	1.10	23.14	36.50	49.57
TS1P	-0.07	10.78	35.49	34.53
TS2P	2.69	21.08	15.87	19.53

[a] See ref 4.

deed, large negative -TΔS values are obtained for the TS's which amount 10-12 kcal·mol^{-1} per water molecule being a little smaller in acid-catalyzed processes.

Though entropic terms are higher for assisted reactions, free energies of activation for these processes remain lower than those obtained for non-assisted mechanisms especially for catalyzed processes (by ~ 8 kcal·mol^{-1} and ~ 20 kcal·mol^{-1} for neutral and protonated reactions respectively). Note finally that BLYP leads to results close to those obtained at MP2/6-31G**//RHF/3-21G. The main difference lies in the stabilizing effect of the bifunctional catalysis which is more important in BLYP.

Conclusions

Qualitatively, semiempirical, DFT and ab initio methods give similar results in the study of amide hydrolysis which is favoured by bifunctional catalysis as it was demonstrated in a previous work [4].

It appears that BLYP/6-31G** reaction mechanisms are more synchronous than those obtained at either MP2/6-31G** or AM1 levels of computation. Contrary to previously reported RHF/3-21G results and AM1 results reported here, the geometry of the transition state corresponding to the neutral water-assisted mechanism (TS2N) is not planar at BLYP and MP2 levels of computation. Concerning the catalyzed water-assisted process (TS2P), all the methods predict similar non-planar structures. In general, BLYP and MP2 geometries are not very different.

AM1, MP2 and BLYP computations predict the effect due to acid and bifunctional catalysis. However, some noticeable differences exist when quantitative aspects are considered. It is noteworthy that BLYP computations seem to enhance the acid catalysis. Free-energy calculations carried out at the BLYP level confirm that assisted mechanisms are favoured with respect to non-assisted ones.

We have not analyzed in this work the role of long-range electrostatic interactions with the solvent but in a previous paper [4] it was shown to be rather small.

One of the main goals of this work was to inspect the suitability of a computational procedure that consists in the optimization of molecular geometries at the AM1 semiempirical level, followed by single-point calculations at ab initio or DFT levels. This procedure would allow the study of peptide hydrolysis in enzymatic processes through the use of hybrid AM1/MM approaches to obtain molecular geometries followed by more accurate DFT or ab initio calculations for selected structures. In this paper, we have shown that this calculation scheme allows to improve a little the results obtained at the AM1 level for the Transition State relative energies. Nevertheless, there are still significant differences with the results obtained using full optimized geometries with ab initio or DFT methods. Therefore, obtaining more accurate results may require to perform QM/MM calculations beyond the semiempirical level. Such calculations are still intractable with traditional ab initio correlated methods but DFT/MM simulations of chemical reactions in complex systems are already feasible [9].

References

1. Oie, T.; Loew, G. H.; Burt, S.K.; Binkley, J.S.; MacElroy, R.D. *J. Am. Chem. Soc.*, **1982**, *104*, 6169.
2. Krug, J.P.; Popelier, P.L.A.; Bader, R.F.W. *J. Phys. Chem.*, **1992**, *96*, 7604.
3. Jensen, J.H.; Baldridge, K.K.; Gordon, M.S. *J. Phys. Chem.*, **1992**, *96*, 8340.
4. Antonczak, S.; Ruiz-López, M.F.; Rivail, J.-L. *J. Am. Chem. Soc.*, **1994**, *116*, 3912.
5. a) Dobbs, K.D.; Dixon, D.A. *J. Phys. Chem.*, **1996**, *100*, 3965; b) Cho, S.J.; Cui, C., Lee, J.Y.; Park, J.K.; Suh, S.B.; Park, J.; Kim, B.H.; Kim, K.S. *J. Org. Chem.*, **1997**, *62*, 4068; c) Hori, K.; Kamimura, A.; Ando, K.; Mizumura, M.; Ihara, Y. *Tetrahedron*, **1997**, *53*, 4317.
6. a) Alex, A.; Clark, T. *J. Comput. Chem*, **1992**, *13*, 704.; b) Pitarch, J.; Ruiz-López, M.F.; Pascual-Ahuir, J.-L.; Silla, E.; Tuñón, I. *J. Phys. Chem.* in press; c) Frau, J.; Donoso, J.; Muñoz, F.; García Blanco, F. *J. Comp. Chem.*, **1991**, *13*, 681 (see also references cited therein); d) Rivail, J.-L.; Loos, M.; Théry, V. *Trends in Ecological Physical Chemistr*y; Bonati, L.; Cosentino, U.; Lasagni, M.; Moro, G.; Pitea, D.; Schiraldi, A. (Eds.), Elsevier, Amsterdam **1993**, p. 17-26; e) Beveridge, A.J.; Heywood, G.C. *J. Mol. Struct. Theochem*, **1994**, *306*, 235; f) Beveridge, A.J.; Heywood, G.C. *Biochemistry*, **1993**, *32*, 3325; Lee, H.; Darden, T.A.; Pedersen, L.G. *J. Am. Chem. Soc.*, **1996**, *118*, 3946.
7. Binkley, J.S.; Pople, J.A.; Hehre, W.J. *J. Am. Chem. Soc.*, **1989**, *102*, 939.

8. a) Gao, J. *Methods and Applications of Combined Quantum Mechanical and Molecular Mechanical Potentials*; Lipkowitz, K.B.; Boyd, D.B. (Eds); VCH Review in Computational Chemistry, Vol. 7 **1996** p. 119-185.; b) Théry, V.; Rinaldi, D.; Rivail, J.-L., Maigret, B.; Ferenczy, G. *J. Comput. Chem.* **1994**, *15*, 269; c) Monard, G.; Loos, M.; Théry, V.; Baka, K.; Rivail, J.-L. *Int. J. Quantum Chem.*, **1996**, *58* , 153.
9. a) Tuñón, I.; Martins-Costa, M.T.C.; Millot, C.; Ruiz-López, M.F. *J. Mol. Mod.* **1995**, *1*, 196; b) Tuñon, I.; Martins-Costa, M.T.C.; Millot, C.; Ruiz-López, M.F. *J. Chem. Phys.* **1997**, *106*, 3633; c) Strnad, M.; Martins-Costa, M.T.C.; Millot, C.; Tuñón, I.; Ruiz-López, M.F.; Rivail, J.-L. *J. Chem. Phys.* **1997**, *106*, 3643.
10. Assfeld, X., Rivail, J.-L. *Chem. Phys. Lett.* **1996**, *263*, 100.
11. Antonczak, S.; Monard, G.; Ruiz-López, M.F.; Loos, M.; Rivail, J.-L. in progress.
12. Ziegler, T. *Chem. Rev.* **1991**, *91*, 651.
13. a) Johnson, J.G.; Gill, P.M.W.; Pople, J.A. *J. Chem. Phys.*, **1993**, *98*, 5612.; b) Andzelm, J.; Wimmer, E. *J. Chem. Phys.*, **1992**, *96*, 1280.; c) Becke, A.D. *J. Chem. Phys.*, **1992**, *96*, 2155.; d) Gill, P.M.W.; Johnson, J.G.; Pople, J.A.; Frisch, M. *J. Chem. Phys. Lett.*, **1992**, *197*, 499; e) Handy, N.C.; Maslen, P.E.; Amos, R.D.; Andrews, J.S. *Chem. Phys. Lett.*, **1992**, *197*, 506; f) Johnson, J.G.; Gill, P.M.W.; Pople, J.A. *J. Chem. Phys.*, **1992**, *97*, 7846; g) Murray, C.W.; Lamming, G.J.; Handy, N.C.; Amos, R.D. *Chem. Phys. Lett.*, **1992**, *199*, 551; h) Gill, P.M.W.; Johnson, J.G.; Pople, J.A.; Frisch, M.J. *Int. J. Quantum Chem. Symp.*, **1992**, *26*, 319; i) Barone, V. *Chem. Phys. Lett.*, **1994**, *226*, 973; j) Barone, V.; *J. Phys. Chem.*, **1994**, *101*, 6834.
14. a) Pullumbi, P.; Mijoule, C.; Manceron, L.; Bouteiller, Y. *Chem. Phys*, **1994**, 185, 13, 25; b) Pullumbi, P.; Bouteiller, Y.; Manceron, L. *J. Chem. Phys.*, **1994**, *101*, 3610.
15. Frish, M.J.; Trucks, G.W.; Head-Gordon, M.; Gill, P.M.W.; Wrong, M.W.; Foresman, J.B.; Johnson, B.G.; Schlegel, H.B.; Robb, M.A.; Reprogle, E.S.; Gomperts, R.; Andres, J.L.; Raghavachari, K.; Binkley, J.S.; Gonzales, C.; Martin, R.L.; Fox, D.J.; Defrees, D.J.; Baker, J.; Stewart, J.J.P.; Pople, J.A. Gaussian 92/DFT, Carnegie-Mellon Quantum Chemistry Publishing Unit, Pittsburgh, PA, **1992**.
16. Francl, M.M.; Pietro, W.J.; Hehre, W.J.; Binkley, J.S.; Gordon, M.S.; DeFrees, J.D.; Pople, J.A. *J. Chem. Phys.*, **1982**, *77*, 3654.
17. Szabo, A; Ostlund, N.S. *Modern Quantum Chemistry: Introduction to Advanced Electronic Structure Theory*; Mcmillan, New-York, **1986**.
18. Becke, A.D. *J. Chem. Phys.*, **1988**, *88*, 2547.
19. Lee, C.; Yang, W.; Parr, R.G. *Phys. Rev. B*, **1988**, *37*, 786.
20. a) Li, J.; Schrekenbach, G.; Ziegler, T. *J. Phys. Chem.*, **1994**, *98*, 4838; b) Gill, P.M.W.; Johnson, B.G.; Pople, J.A. *Chem. Phys. Lett.*, **1993**, *209*, 506; c) Smith, B. J.; Radom, L. *Chem. Phys. Lett.*, **1994**, *231*, 345.
21. Rinaldi, D.; Hoggan, P.E.; Cartier, A GEOMOS: Semi-Empirical SCF System for Dealing with Solvent Effects and Solid Surface Adsorption (QCPE 584a), QCPE Bull. **1989**, 128.
22. Dewar, M.J.S.; Zoebisch, E.G.; Healy, E.F.; Stewart, J.J.P. *J. Am. Chem. Soc.*, **1985**, *107*, 3902.
23. Schlegel, H.B. *J. Comput. Chem.*, **1982**, *3*, 214.
24. Hehre, W.J.; Radom, L.; Schleyer, P.v.R.; Pople, J.A. *Ab Initio Molecular Orbital Theory*; Wiley, J. & Sons, New-York, **1986**, p. 226-261.
25. Wiest, O.; Houk, K.N. *Topics Curr. Chem.*, **1996**, *183*, 1.
26. Zhang, Q.; Bell, R.; Truong, T.N. *J. Phys. Chem.*, **1995**, *99*, 592.
27. a) González, L.; Mó, O.; Yáñez, M.; Elguero, J. *J. Mol. Struct. Theochem*, **1996**, *371*, 1; b) Novoa, J.J.; Mota, F.; Perez del Valle, C.; Planas, Marc, *J. Phys. Chem*, in press.